

MODIS STATISTICAL STRUCTURE FUNCTION ANALYSIS

Tomoko Koyama*, Donald W. Hillger, and Thomas H. Vonder Haar
 Cooperative Institute for Research in the Atmosphere/Department of Atmospheric Science
 Colorado State University, Fort Collins, Colorado

1. Introduction

The Moderate Resolution Imaging Spectroradiometer (MODIS) is the key instrument aboard the Terra (EOS AM-1) satellite. Terra MODIS views the entire Earth's surface every 1 to 2 days, acquiring data in 36 spectral bands (0.4 μm - 14.5 μm). It not only has more bands than the heritage instruments like the AVHRR or the HIRS, but also better resolution such as 250, 500 and 1000 m at nadir. It provides key observations important to study of atmosphere, oceans, and land surfaces with emphasis on interactions between each of the systems. The goal of this study is to estimate noise levels of the MODIS Thermal Emissive Bands (TEB) using spatial structure analysis. The target bands are bands 20 to 36 except band 26 (see Table 1 below).

TABLE 1
 MODIS Spectral Bands

Primary Use	Band	Bandwidth (μm)
Surface/Cloud Temperature	20	3.8819 - 3.6915
	21	4.0343 - 3.9505
	22	4.0158 - 3.9287
	23	4.1008 - 4.0139
Atmospheric Temperature	24	4.5191 - 4.4280
	25	4.5921 - 4.4999
Water Vapor	27	6.8868 - 6.6461
	28	7.5078 - 7.1831
	29	8.7066 - 8.3574
Ozone	30	9.8956 - 9.5946
Surface/Cloud Temperature	31	11.2797 - 10.7591
	32	12.3009 - 11.7779
Cloud Top Altitude	33	13.5217 - 13.2127
	34	13.8475 - 13.5217
	35	14.0795 - 13.7504
	36	14.3421 - 14.0558

2. Methodology

Statistical structure function was used by Gandin (1963) in an objective analysis technique.

*Corresponding author address: Tomoko Koyama, Dept. of Atmospheric Science, Colorado State University, Fort Collins, CO 80523;
 e-mail: koyama@cira.colostate.edu

The structure function (STR) of quantity *f* at each of the two points \hat{r}_1 and \hat{r}_2 is given by:

$$STR(\hat{r}_1, \hat{r}_2) = N^{-1} \sum [f'(\hat{r}_1) - f'(\hat{r}_2)]^2$$

where

$$f'(\hat{r}) = f(\hat{r}) - \bar{f}(\hat{r})$$

and \bar{f} is the mean over time for *N* observations at each point. This function approaches twice the inherent variance of the measuring system as the data separation approaches zero.

$$STR(\rho = 0) = 2\sigma^2$$

When scalar separation distance can be expressed as:

$$\rho = |\hat{r}_1 - \hat{r}_2|$$

Estimates of STR(0) can be obtained by extrapolating the structure values to zero separation, and structure-derived uncertainties as a result do not include any type of bias or systematic error.

For the error estimation, two assumptions are required, no cloud contaminated and spatially homogeneous field. When these conditions are satisfied, the structure function will be independent of the position and orientation of the pair of observations. Each 1-km resolution band has a ten-element linear detector array. Thus, along line (Track-direction) analysis shows a single detector performance, whereas along element (Scan-direction) gives us structure values of the entire array of detectors for each band (see Figure 1 below).

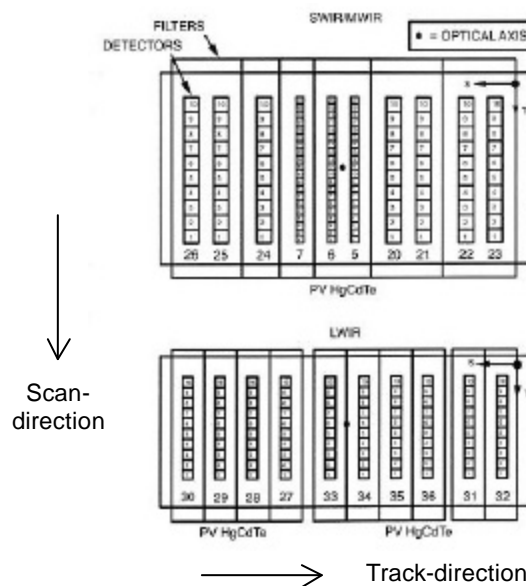


Figure 1. Focal plane

3. Data

Two data products of MODIS are used in this study.

3.1 Calibrated radiances 1 km (MOD021KM)

Three “Calibrated radiances 1 km” datasets are used for this study. They contain calibrated and geolocated radiances for 36 bands generated from MODIS Level 1A sensor counts. They are generated and distributed from NASA/GSFC and the target bands have 1-km resolution at nadir. Several cloud-free areas (51 x 51 grid size) for the structure function analysis from each data set were determined on a McIDAS system. Cloud clearing was performed manually using all bands.

3.2 Cloud mask (MOD35_L2)

Because different cloud types reflect and emit radiant energy differently, we can use MODIS' unique data set to distinguish between water, snow, and ice clouds. To satisfy the assumption for the structure function analysis, cloud mask product is used as ancillary information. MODIS cloud mask is more than a simple yes/no decision. Only two flags from the cloud mask product are used in this study. The first one identifies the algorithm success, and the second one describes the cloud obstruction.

Figure 2 shows statistical information of one analysis area (26 x 26 grids), mean equivalent blackbody temperature and its standard deviation. Solid lines show the whole coverage results, and the other lines show one-dimensional results having the same center position. Percentages in the legend are confident/probably clear grid ratio derived from the cloud mask product. A homogeneous and uniform observation field is required for the structure function analysis; on the other hand, a real observation field will never achieve such a perfect condition. However, the variability of this scene is small enough and standard deviations could be regarded as the maximum errors of the analyzed region.

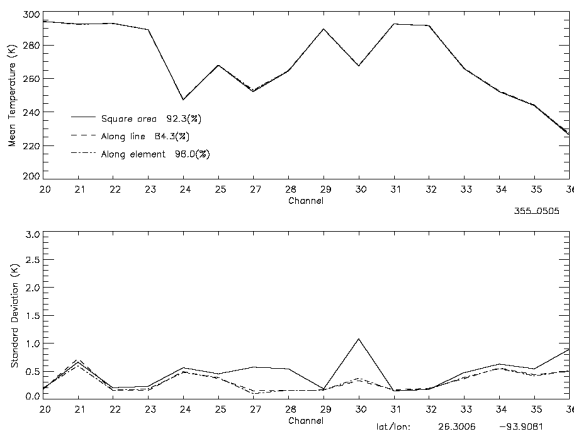


Figure 2. Mean Tbb and its standard deviation of an analysis area

4. Trade-off problem – Extrapolating the structure function

It is critical to find a fitted function to extrapolate the structure function to zero distance for the error evaluation. The coefficient of determination (C.O.D.) as an indicator is introduced to get appropriate estimations in this study. The C.O.D. varies from 0 to 1 and reveals how closely the trend line fits to the actual data. By decreasing the spatial sampling area, a trend line fits to observations better. Therefore, there is a trade-off problem to extrapolate the structure value at zero separation distance to determine error values:

- Does the trend line fit to the observation points well?
- Does the fitted curve show the inherence of the whole analysis area sufficiently?

Figure 3 shows three kinds of fitting curves (polynomial functions) as the result of six different C.O.D.s as the thresholds. The black points in the following figures are the structure function values for a case of the band 31, Track-direction analysis. Also, solid, dotted, and dashed lines show the second, the third, and the fourth order polynomials respectively. From the figures, we can see higher C.O.D. as a threshold can give us more uniform error estimation. The numbers that appears in the upper left part of the graphs are the number of points that were used to achieve the C.O.D. from left to right, the numbers correspond to the second, third and fourth order polynomials, respectively.

5. What makes the error bigger?

Because of the MODIS design, striped images can be found on several band's scenes, which would affect the result of Scan-direction analysis. This effect could be caused by:

- 1) Non-Functioning Detectors
- 2) Incomplete knowledge of sensor response across scan Thermal Emissive Bands (bands 20-36, except band 26)
- 3) Non-uniform channel to channel response within a band (bands 20-25)

and so on. Also, radiance error might exist due to Optical cross-talk from band 31 into band 32 through 36 optical leak causes scattering off a spectral filter edge. For the difference between Scan-direction and Track-direction analyses, we have to consider characterization of the instrument spatial response profile or line spread function (LSF), causing image blur with most bands (See Figure 4).

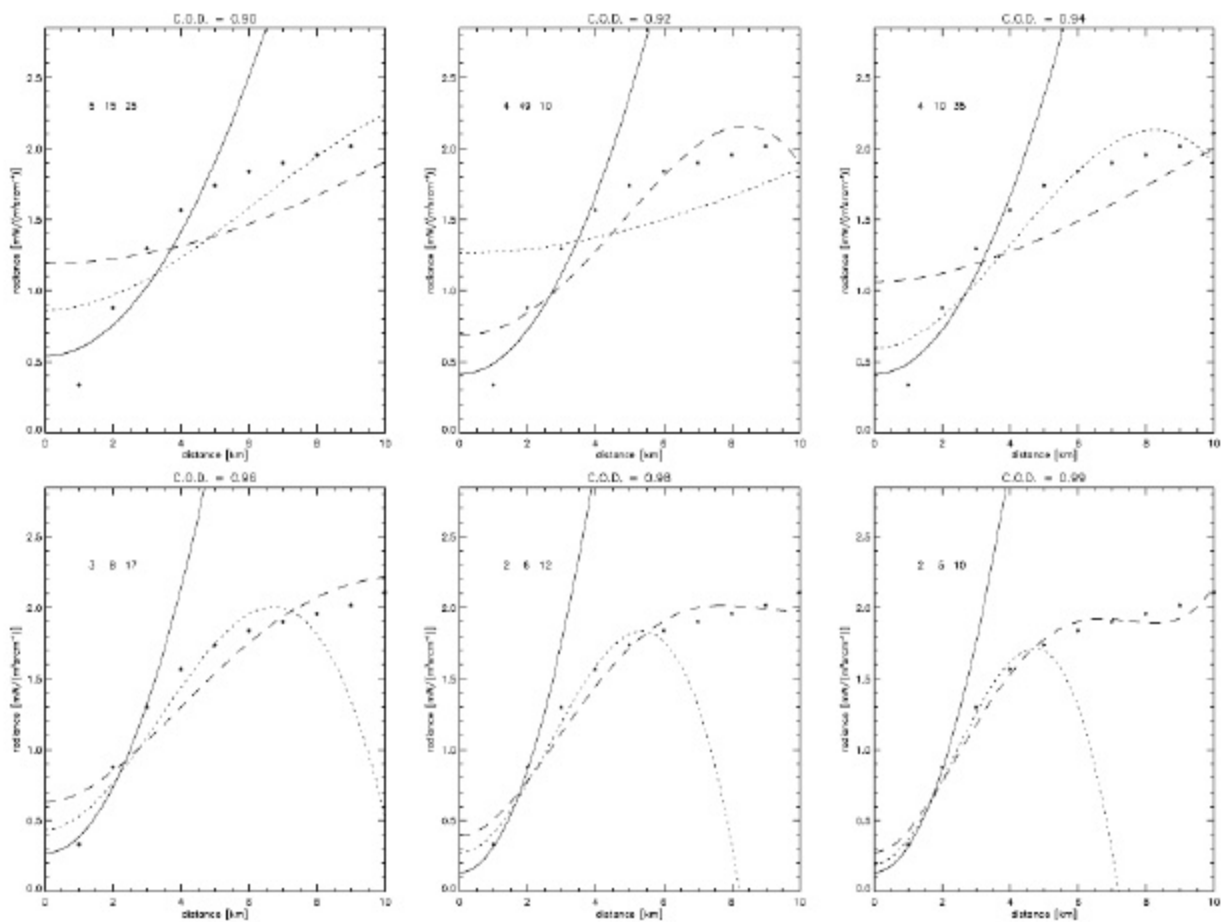


Figure 3. Structure function values and the fitting curves by different C.O.D.s

6. Preliminary results

Table 2 shows Noise-equivalent temperature difference (NE Δ T) values of the pre-launch study and those derived from the structure function analysis.

“Spec” column shows the required MODIS sensitivities, and “Line” and “Element” are the results from Track-direction and Scan-direction analysis respectively. “Pre-launch” testing program was executed on the MODIS Protoflight Model (PFM). Those values are estimates taken from channel 5 (the fifth detector, in the middle of each ten detector array) of each band. Thus, the NE Δ T values do not include the effects of striping.

The two values of “Line” and “Element” columns show the minimum and the maximum values of the 6 smallest values from 60 case studies. Due to the digitization limit, there are unavoidable errors at the asterisked 0.000. But they are very small numbers (.0001 - .0062 K, assuming typical Earth scene for each

band). Shaded boxes are “striped” images recognized evidently.

In general, the shorter wavelength bands show larger errors than the pre-launch values. There are several reasons that cause the uncertainty as mentioned before. However, the attraction of this technique is that it does not require comparisons with another data source to estimate errors.

7. Acknowledgement

Mr. Chris Moeller at CIMSS, University of Wisconsin provided McIDAS formatted MODIS Calibrated radiances 1km and useful information about the research. This work was supported by NOAA Grant NA17RJ122B.

9. World Wide Web links

MODIS Web page:
<http://ftpwww.gsfc.nasa.gov/MODIS/MODIS.html>
 MODIS Characterization Support Team (MCST):
<http://mcstweb.gsfc.nasa.gov/>
 DAAC Data Sets:
<http://eosdata.gsfc.nasa.gov/data/dataset/index.html>

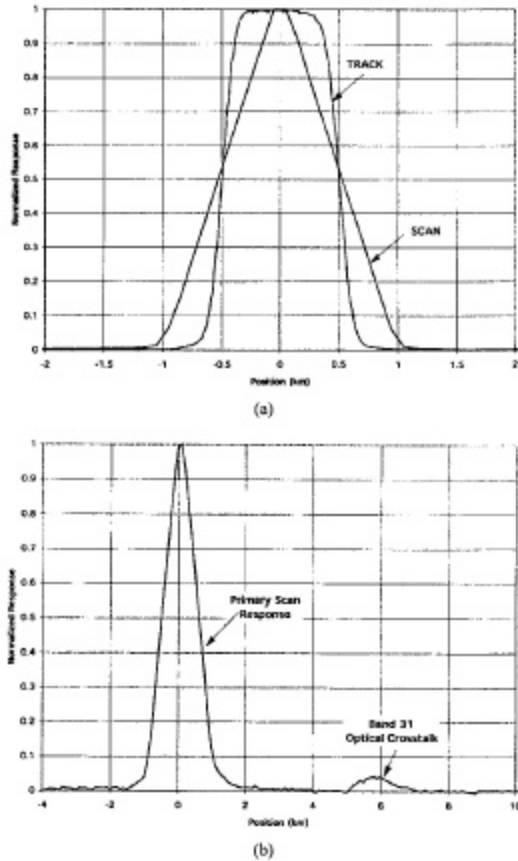


Figure 4. Typical LSF's for MODIS. (a) Band 10, channel 6. (b) Band 35 has a ~5% leak in the region of band 31 in the scan direction.

8. References

Ackerman, S. A., K. I. Strabala, W.P. Menzel, R. A. Fray, C.C. Moeller, and L. E. Gumley, 1998: Discriminating clear sky from clouds with MODIS. *J. Geophys. Res.*, 103, 32141-32157.
 Barnes, W. L., T. S. Pagano, and V.V. Salomonson, 1998: Prelaunch characteristics of the Moderate Resolution Imaging Spectroradiometer (MODIS) on EOS-AM1. *IEEE Trans. Geosci. Remote Sensing*, 36, 1088-1100.
 Gandin, L.S., 1963: Objective analysis of meteorological fields. Translated from Russian, Israel Program for Scientific Translation, Jerusalem, 242pp.
 Hillger, D.W., and T. H. Vonder Haar, 1979: An analysis of satellite infrared soundings at the mesoscale using statistical structure and correlation functions. *J. Atmos. Sci.*, 36, 287-305.
 Hillger, D.W., and T. H. Vonder Haar, 1988: Estimating noise levels of remotely sensed measurements from satellites using spatial structure analysis. *J. Atmos. Ocean. Tech.*, 5, 206-214.

Table 2
 NE Δ T comparison (K)

Band	Spec	Line	Element	Pre-launch
20	0.05	0.260 ~ 0.415	0.248 ~ 0.401	0.027
21	2.00	0.336 ~ 0.520	0.405 ~ 0.617	0.155
22	0.07	0.246 ~ 0.405	0.280 ~ 0.405	0.027
23	0.07	0.215 ~ 0.363	0.249 ~ 0.382	0.025
24	0.25	0.054 ~ 0.112	0.000* ~ 0.099	0.126
25	0.25	0.129 ~ 0.212	0.000* ~ 0.163	0.060
27	0.25	0.011 ~ 0.054	0.100 ~ 0.147	0.097
28	0.25	0.010 ~ 0.162	0.000* ~ 0.131	0.043
29	0.05	0.150 ~ 0.363	0.000* ~ 0.298	0.020
30	0.25	0.113 ~ 0.205	0.200 ~ 0.448	0.086
31	0.05	0.151 ~ 0.392	0.000* ~ 0.331	0.026
32	0.05	0.135 ~ 0.387	0.000* ~ 0.381	0.039
33	0.25	0.097 ~ 0.217	0.198 ~ 0.348	0.135
34	0.25	0.081 ~ 0.133	0.099 ~ 0.139	0.200
35	0.25	0.082 ~ 0.121	0.108 ~ 0.126	0.232
36	0.35	0.000* ~ 0.148	0.181 ~ 0.223	0.457